THE JOURNAL OF PHYSICAL CHEMISTRY C

Article

pubs.acs.org/JPCC

Resistive Switching Induced by Electric Pulses in a Single-Component Molecular Mott Insulator

Pablo Stoliar,[†,∥] Pascale Diener,[†] Julien Tranchant,[†] Benoît Corraze,[*,†] Benjamin Brière,[‡] Vinh Ta-Phuoc,[‡] Nathalie Bellec,[§] Marc Fourmigué,[§] Dominique Lorcy,[*,§] Etienne Janod,[†] and Laurent Cario[†]

[†]Institut des Matériaux Jean Rouxel, CNRS Université de Nantes, UMR 6502, BP32229, 44322 Nantes, France

[‡]GREMAN UMR 7347 CNRS, Université F. Rabelais, Parc de Grandmont, 37200 Tours, France

[§]Institut des Sciences Chimiques de Rennes, Université Rennes 1, UMR CNRS 6226, 35042 Rennes, France

ABSTRACT: Resistive random-access memory (ReRAM) made of organic materials has recently received much attention for application in flexible devices. In the latter, resistive switching is usually obtained thanks to electrochemical effects or charge trapping. This work shows that, under electric pulses, the crystalline molecular Mott insulator [Au(Et-thiazdt)$_2$] exhibits a resistive switching based on an insulator-to-metal transition (IMT). Electric pulses exceeding a threshold electric field of a few kilovolts/centimeter induce a volatile transition, due to an intrinsic, purely electronic effect related to an avalanche phenomenon. Moreover, the application of electric pulses of higher amplitude induces a nonvolatile and reversible resistive switching. Both two-level and multilevel switching between resistances R_{on} and R_{off} are observed. At room temperature, a R_{off}/R_{on} ratio >100 is obtained, which is very high for this kind of switching mechanism and quite promising for ReRAM applications. [Au(Et-thiazdt)$_2$] appears as the first molecular member of a new class of ReRAM called Mott memories.

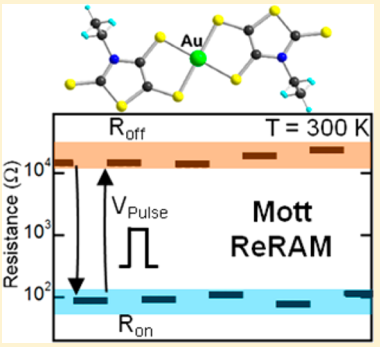

INTRODUCTION

The demand for organic-based electronic devices has recently increased due to their potential advantages over conventional inorganic electronics, such as their low fabrication cost, high mechanical flexibility, light weight, and ease of fabrication.[1,2] Flexible organic memories that would enable data processing, storage, and communication are essential components to achieve flexible electronics.[3−9] In that context, resistive random-access memory (ReRAM) made of organic materials has recently received much attention.[10−14] In ReRAM, information storage is enabled by a nonvolatile resistive switching between two different resistance states achieved by the application of short electric pulses. In organic ReRAM, resistive switching mechanisms generally involve electrochemical effects associated with anion or cation migrations or charge trapping in metallic nanoparticles.[15−20] A new type of resistive switching was recently reported in several chalcogenide inorganic narrow-gap Mott insulators with formulation AM_4Q_8 (A = Ga, Ge; M = V, Nb, Ta; Q = S, Se).[21−24] The application of short electric pulses on these compounds induces a new phenomenon of volatile and nonvolatile resistive switching related to the collapse of the Mott insulating state. The volatile transition appears above threshold electric fields of a few kilovolts/centimeter and is based on an electronic avalanche process.[22,23] For electric fields much higher than the threshold avalanche breakdown field (E_{th}), the resistive switching turns nonvolatile.[21] The switching mechanism is closely related with their Mott insulator character, as the avalanche breakdown induces the collapse of the Mott insulating state at the local scale and triggers the formation of a granular conductive filament formed by metallic and superinsulating domains.[21−23,25] First identified in inorganic compounds, the generalization of this purely electronic intrinsic effect to *organic* Mott insulators could open new perspectives in organic electronics. Such compounds can be found in mixed valence, multicomponent salts derived from tetrathiafulvalenes or from metal bis(dithiolene) complexes, for example, the conducting C[M(dmit)$_2$]$_2$ salts (dmit = 1,3-dithiole-2-thione-4,5-dithiolate, C = TTF$^+$, Me$_4$N$^+$, ...).[26,27] More recently, *single-component* molecular conductors based on neutral metal bis(dithiolene) complexes have also emerged as attractive systems devoid of any counterions.[28−30] For instance, neutral gold complexes formulated as [Au(dt)$_2$]$^\bullet$ are radical species and can potentially behave as Mott insulators, with one radical per site.[31−33] The possible observation of a resistive switching phenomenon among such molecular compounds is addressed here. We will show, indeed, that the application of electric pulses on the neutral gold dithiolene complex [Au(Et-thiazdt)$_2$]$^\bullet$, behaving as a molecular Mott insulator (Figure 1), actually follows all features that characterize a Mott-type resistive switching, which is of potential interest for ReRAM applications.

RESULTS AND DISCUSSION

The Narrow-Gap Mott Insulator [Au(Et-thiazdt)$_2$]. We recently reported that the neutral radical complex [Au(Et-thiazdt)$_2$]$^\bullet$ (Et-thiazdt = *N*-ethyl-1,3-thiazoline-2-thione-4,5-dithiolate) adopts a layered structure,[34,35] with uniform stacks

Received: December 23, 2014
Published: January 21, 2015

DOI: 10.1021/jp512810e
J. Phys. Chem. C 2015, 119, 2983−2988

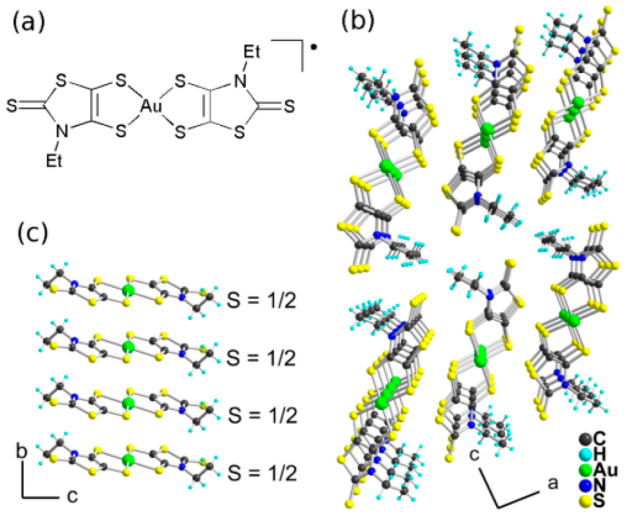

Figure 1. Structure of the neutral radical $[Au(Et\text{-}thiazdt)_2]$. (a) Chemical structure. (b) Solid-state organization. (c) Detail of a chain of radicals running along b; each complex carries a spin $S = {}^1/_2$.

of radical complexes running along b and interacting laterally along a (Figure 1). As the chains are not dimerized, each complex acts as a site with spin $S = {}^1/_2$ (Figure 1c).[34,35] Therefore, this compound is a magnetic narrow-gap insulator with one unpaired electron per site and can be classified as a Mott insulator.

In order to confirm the Mott insulating state, the resistivity of a crystal of $[Au(Et\text{-}thiazdt)_2]$ was reinvestigated. Resistivity measurements performed on single crystals show an activated behavior $\rho = \rho_0 \exp(E_a/kT)$ consistent with a gap $E_g = 2E_a \approx 0.23$ eV (Figure 2a).[34,35] In addition, optical spectroscopy measurements were performed on other crystals of the same batch (Figure 2b). Apart from phonon modes below 1500 cm^{-1}, the optical conductivity spectrum displays an onset at 0.24 eV, in very good agreement with the gap value extracted from transport experiments. This is a clear demonstration of the insulating nature of $[Au(Et\text{-}thiazdt)_2]$, which fully supports a Mott insulating state with a narrow Mott−Hubbard gap of 0.23−0.24 eV.

Resistive Switching Experiments. A comprehensive set of volatile and nonvolatile resistive switching experiments was carried out on single crystals of $[Au(Et\text{-}thiazdt)_2]$.

Volatile Resistive Switching. The volatile resistive switching in inorganic narrow-gap Mott insulators is characterized by two main features:[21−23] (1) a sudden drop of the resistance during an applied pulse exceeding a threshold electric field E_{th} in the 1−10 kV/cm range and appearing after a delay t_{delay} that decreases as the voltage pulse increases (after the pulse, the resistance of the sample goes back to its initial value) and (2) an $I(V)$ characteristic with two distinctive parts. The first one for the nontransited state follows an ohmic law. The second one, which is almost vertical and lies at E_{th}, stands for the transited state. Both t_{delay} and $I(V)$ characteristics are fingerprints of the avalanche breakdown in narrow-gap Mott insulators.[21−23] Following those lines, we have investigated single crystals of $[Au(Et\text{-}thiazdt)_2]$. Parts a, b, and c of Figure 3 display, respectively, the resistance $[R(t)]$, the current $[I(t)]$, and the sample voltage $[V_s(t)]$ measured for crystal A (interelectrode distance $d = 25$ μm, sample section $S = 50 \times 20$ μm^2) during the application of a series of short (200 μs) voltage pulses at 160 K. These experiments were performed

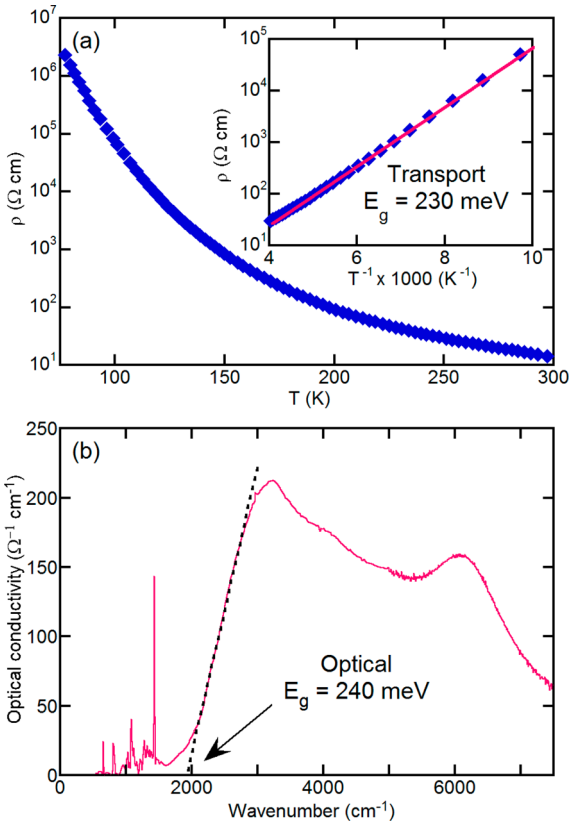

Figure 2. (a) Resistivity as a function of temperature. The inset shows the same data as a function of inverse temperature, and the solid line is the fit with an activation law with a gap E_g. (b) Optical conductivity at ambient temperature. The dotted line indicates the procedure used to determine the optical gap.

using a simple circuit made of the crystal connected in series with a load resistor to a pulse generator (Figure 3d). An abrupt current increase and a voltage decrease across the sample are observed for applied voltages that exceed a threshold voltage $V_{th} = 16.5$ V, shown as a black dotted line in Figure 3c.

These transitions correspond to volatile resistive switching from a high to a low resistance state (Figure 3a). Indeed, after the release of the voltage across the sample, the resistance goes back to its initial high resistance state. Moreover, the resistive switching occurs at a time t_{delay} after the beginning of the pulse. t_{delay} decreases (from 200 to 1 μs in the example displayed in Figure 3a) as the voltage across the sample increases. Furthermore, the sample voltage (V_s) after the resistive switching in $[Au(Et\text{-}thiazdt)_2]$ has always the same value, $V_{th} \approx 16.5$ V, whatever the applied voltage is (Figure 3c,e). As a consequence, the $I(V)$ characteristic in the transited state is almost a vertical line (Figure 3e) that lies at the threshold voltage V_{th} that also corresponds to the lower voltage inducing a resistive switching in dc measurements (Figure 3e). A threshold field $E_{th} \approx 2.5$ kV/cm is obtained at 160 K by properly subtracting the contact resistances (see the Experimental Section). A small decrease of the threshold field is observed by increasing the temperature to 300 K (down to 1 kV/cm).[36] The behavior of $[Au(Et\text{-}thiazdt)_2]$ under electric pulses and the $I-V$ characteristics are remarkably similar to the results reported for the narrow-gap AM_4Q_8 compounds.[21−23] At this step, it is already clear that the volatile resistive switching observed here in $[Au(Et\text{-}thiazdt)_2]$ cannot be explained by purely nonvolatile resistive switching processes,

DOI: 10.1021/jp512810e
J. Phys. Chem. C 2015, 119, 2983−2988

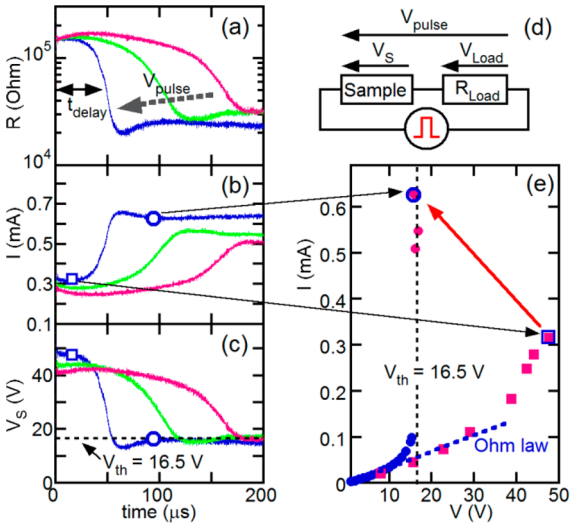

Figure 3. Volatile resistive switching observed at 160 K on [Au(Et-thiazdt)$_2$], data obtained on sample A. (a) Resistance, (b) current, and (c) voltage evolution during electric pulses of three different amplitudes V_{pulse} (70, 75, and 82 V), showing that t_{delay} decreases with increasing V_{pulse}. (d) Schematic of the experimental setup. (e) $I-V$ characteristics. The I and V values before (square) and after (circle) the resistive switching contributes to two distinct $I-V$ branches (see the text). The results obtained with a standard dc technique are also indicated (blue dots) and the blue dotted line shows the ohmic behavior. The black dotted line in parts c and e corresponds to the threshold voltage, V_{th}.

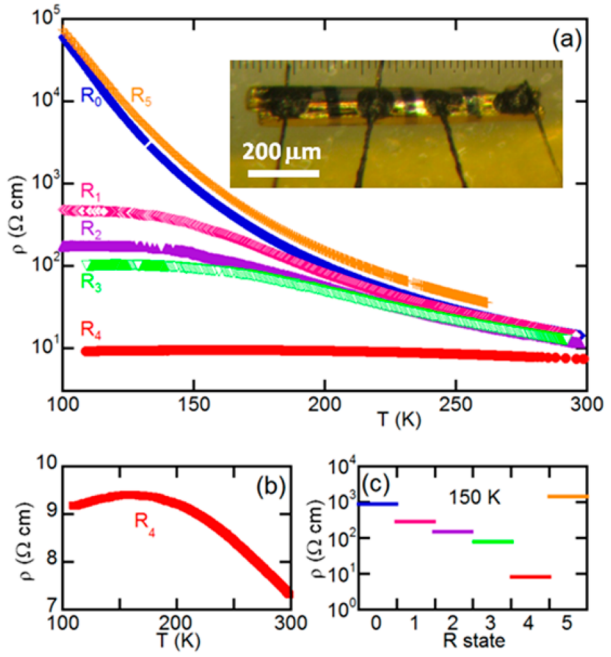

Figure 4. (a) Temperature dependence of the resistivity along the b-axis before and after successive nonvolatile switches at 150 K. R_0 indicates the pristine state, R_1 (R_2, R_3, R_4, and R_5) is measured after the first (respectively second, third, fourth, and fifth) nonvolatile switching. The inset is a photograph of the single crystal with the four gold contacts. (b) The curve R_4 is shown in a linear scale to magnify the metallic behavior at low temperature. (c) Resistivity at 150 K in the successive resistance states. Data obtained from sample B.

such as electrochemical or thermochemical mechanisms.[37−39] On the other hand, the magnitude of the threshold field in [Au(Et-thiazdt)$_2$] compares well with the value of 1 kV/cm observed for avalanche breakdown in the narrow-gap semiconductor InSb.[40,41] This comparison strongly supports an electronic avalanche mechanism as the common origin of the resistive switching for all these compounds. In addition, we note that very similar $I(V)$ characteristics were recently reported in another, but multicomponent, organic Mott insulator formulated as κ-(BEDT-TTF)$_2$Cu[N(CN)$_2$]Br by a combination of external electric field and photoirradiation.[42]

Nonvolatile Resistive Switching. Figure 4a shows four-probe resistivity measurements as a function of temperature [$\rho(T)$] of crystal B (d = 35 μm, S = 60 × 60 μm^2) before and after applying at 150 K a series of short electric pulses of amplitude sufficiently higher than E_{th} to generate the nonvolatile transition. The application of these electric pulses induces a nonvolatile decrease of the resistivity $\rho(T)$ by more than 3 orders of magnitude at low temperature (110 K). The different curves of Figure 4a correspond to the low bias (lower than 0.01 V) resistivity after different electric pulses. Curve R_0 gives the resistivity of the pristine Mott insulating state before the application of any electric pulse. A nonvolatile resistive switching is obtained for an electric field typically exceeding $4E_{th}$. The resistive switching is initiated by a burst of 20 pulses (amplitude $E = 4E_{th}$, duration t_{on} = 50 μs, and period t_{off} = 1 ms) at 150 K. It leads to the low bias resistivity curve (R_1) showing a drop in resistivity by 2 orders of magnitude at 100 K. The application of further identical bursts reduces the resistivity by up to 3 orders of magnitude at low temperature (curves R_2-R_4 in Figure 4a).

The temperature dependence of all these transited states (curves R_1-R_3 in Figure 4a) is consistent with a two channel transport behavior mimicking granular metallic filamentary paths reinforced at every pulse and embedded in a pristinelike matrix.[43] Moreover, a metallic behavior is even observed for curve R_4 below 150 K (Figure 4b), which suggests that in [Au(Et-thiazdt)$_2$] even a percolating metallic filamentary path is achievable. Note finally that the last single pulse with the same polarity but lower electric field and higher time (E = 1.3E_{th}, t_{on} = 400 μs), which favors Joule heating, is able to switch back the resistivity to a high resistance state close to the pristine value (curve R_5). This transition to the high resistance state is fully consistent with a thermal-based reset transition, as suggested by our modeling of the transition.[22,23] Moreover, the control of the set and reset transitions enables one to switch back and forth reproducibly between high and low resistance states.[44] Figure 5 gives an example of such successive resistive switching observed on another much thinner crystal of [Au(Et-thiazdt)$_2$] (crystal C, d = 35 μm, S = 40 × 10 μm^2) at room temperature.

A burst of seven pulses ($E = 4E_{th}$, t_{on} = 30 μs, and t_{off} = 200 μs) is applied to switch from the R_{off} to R_{on} state; the resistance is switched back to R_{off} by applying one longer pulse ($E = 1.3E_{th}$ and t_{on} = 200 μs). It shows a R_{off}/R_{on} ratio higher than 2 orders of magnitude at room temperature (see Figure 5). The difference observed at room temperature for the two different crystals (Figures 4 and 5) is a direct consequence of the filamentary conduction in the low resistance state.[43] The resistance ratio increases from 2 to 100 as the sample section S perpendicular to the current decreases by almost 1 order of magnitude from 60 × 60 to 40 × 10 μm^2. This enhancement of R_{off}/R_{on} with $1/S$ is expected if the resistive switching involves the creation/full dissolution of a single conductive filament. In

DOI: 10.1021/jp512810e
J. Phys. Chem. C 2015, 119, 2983−2988

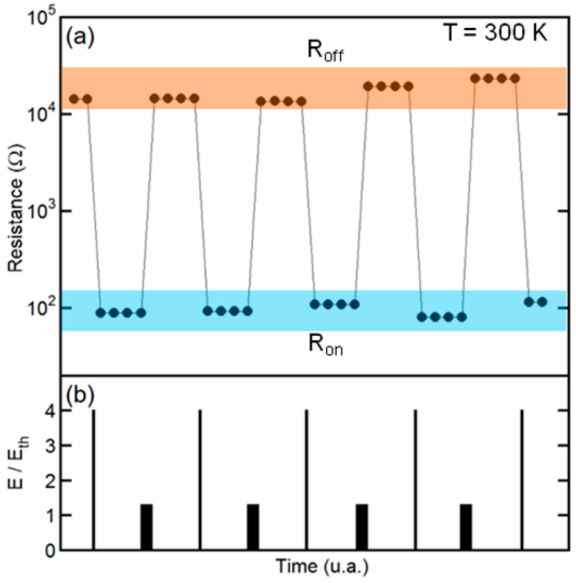

Figure 5. (a) Resistive switching sequence between The R_{on} and R_{off} state at ambient temperature. (b) Amplitude of the unipolar pulses applied during the same sequence. Data obtained from sample C.

this limit, R_{on} is mainly driven by the filament conductance and is independent of the section S, whereas R_{off} increases with $1/S$. This illustrates the remarkable down-scaling potential of $[Au(Et\text{-}thiazdt)_2]$ for possible future organic memories.

■ CONCLUSION

In conclusion, we have found that the organic Mott insulator $[Au(Et\text{-}thiazdt)_2]$ exhibits a resistive switching based on a purely electronic intrinsic effect. This compound undergoes a volatile transition for electric pulses exceeding a threshold electric field of a few kilovolts/centimeter. For electric pulses of amplitude higher than $E = 4E_{th}$, a nonvolatile reversible resistive switching is observed. The phenomenology of the resistive switching observed in $[Au(Et\text{-}thiazdt)_2]$ is similar to that observed in inorganic narrow-gap Mott insulator compounds. $[Au(Et\text{-}thiazdt)_2]$ is therefore the first example of a molecular compound belonging to the class of Mott memories. A R_{off}/R_{on} ratio exceeding 100 is reported at room temperature, well above the ITRS requirements for ReRAM applications ($R_{off}/R_{on} > 10$).[45] This supports that organic Mott insulators are of strong interest in the design of a new type of organic memory.

■ EXPERIMENTAL SECTION

Sample Synthesis. The neutral radical complex $[Au(Et\text{-}thiazdt)_2]$ is obtained as single crystals upon electrocrystallization of its monoanionic precursor, $[Au(Et\text{-}thiazdt)_2]^-$, as the Et_4N^+ salt.[34,35] For this study all single crystals were selected from the same bath.

Optical Measurements. Near normal incidence reflectivity spectra were measured on the 50 × 50 μm^2 mirrorlike surface of several single crystals, using a BRUKER IFS 66v/S and a homemade vacuum microscope in the range 550−11 000 cm^{-1}. After the initial measurement, the samples were coated with a silver film of 150 nm and measured again. These additional data were used as reference mirrors to calculate the reflectivity in order to take into account light scattering on the surface of the sample and possible misalignement. Optical conductivity spectra were obtained consistently by both Kramers−Kronig analysis and Drude−Lorentz fit procedure. The measurements obtained on all the investigated samples gave the same results.

Sample Wiring for Electric Measurements. Gold pads are evaporated on the crystal through a mechanical mask. The pads are contacted using 10 μm gold wires and carbon paste (Electrodag PR-406); see the picture in Figure 4a. The carbon paste is dried at room temperature for several hours. The contact resistance obtained is typically on the order of the sample resistance. This requires a correction of the threshold field described below.

Resistivity Measurements. The resistance versus temperature characteristics were measured using a Keithley 236 in four-probe configuration. During these low-bias measurements, the total voltage applied to the sample did not exceed 10^{-2} V.

Pulse Experiments. Pulse experiments are performed by applying voltage pulses using an Agilent 8114A connected to the circuit schematized in Figure 3e, where the sample was placed in series with a load resistance. Between the pulses, the low-bias resistance is measured using a Keithley 6430. During the pulse, the voltage and current across the sample are measured with a Tektronix DPO3034 oscilloscope associated with a IeS-ISSD210 differential probe.

Determination of the Corrected Threshold Field. The contact resistances are determined by measuring the sample resistance in both four-point and two-point geometry. The measured threshold voltage, corresponding to the voltage of the crystal in series with the contact resistances, is corrected to account for the crystal only. The threshold field is obtained by dividing the corrected voltage by the interelectrode distance.

■ AUTHOR INFORMATION

Corresponding Authors

*B.C. e-mail: benoit.corraze@cnrs-imn.fr.
*D.L. e-mail: dominique.lorcy@univ-rennes1.fr.

Present Address

∥CIC nanoGUNE, 20018 Donostia-San Sebastián, Basque Country, Spain.

Notes

The authors declare no competing financial interest.

■ ACKNOWLEDGMENTS

This work was supported by the ANR (France) under project GOLD-RRAM no. 12-BS07-0032. We also thank the Rennes-Nantes Materials Program supported jointly by CNRS, the Universities of Rennes and Nantes, and the Régions Bretagne and Pays de la Loire. Some parts of this work were also supported by Région Centre−Synchrotron SOLEIL program. P.S. acknowledges the support of the Spanish Ministry of Economy through the Ramón y Cajal (RYC-2012-01031) program.

■ REFERENCES

(1) Kim, J. Y.; Lee, K.; Coates, N. E.; Moses, D.; Nguyen, T.-Q.; Dante, M.; Heeger, A. J. Efficient Tandem Polymer Solar Cells Fabricated by All-Solution Processing. *Science* **2007**, *317*, 222−225.

(2) Na, S.-I.; Kim, S.-S.; Jo, J.; Kim, D.-Y. Efficient and Flexible ITO-Free Organic Solar Cells Using Highly Conductive Polymer Anodes. *Adv. Mater.* **2008**, *20*, 4061−4067.

(3) Ling, Q.-D.; Liaw, D.-J.; Zhu, C.; Chan, D. S.-H.; Kang, E.-T.; Neoh, K.-G. Polymer Electronic Memories: Materials, Devices and Mechanisms. *Prog. Polym. Sci.* **2008**, *33*, 917−978.

DOI: 10.1021/jp512810e
J. Phys. Chem. C 2015, 119, 2983−2988

(4) Ji, Y.; Cho, B.; Song, S.; Kim, T.-W.; Choe, M.; Kahng, Y. H.; Lee, T. Stable Switching Characteristics of Organic Nonvolatile Memory on a Bent Flexible Substrate. *Adv. Mater.* **2010**, *22*, 3071−3075.
(5) Yang, Y.; Ouyang, J.; Ma, L.; Tseng, R. J.-H.; Chu, C.-W. Electrical Switching and Bistability in Organic/Polymeric Thin Films and Memory Devices. *Adv. Funct. Mater.* **2006**, *16*, 1001−1014.
(6) Sekitani, T.; Yokota, T.; Zschieschang, U.; Klauk, H.; Bauer, S.; Takeuchi, K.; Takamiya, M.; Sakurai, T.; Someya, T. Organic Nonvolatile Memory Transistors for Flexible Sensor Arrays. *Science* **2009**, *326*, 1516−1519.
(7) Scott, J. C.; Bozano, L. D. Nonvolatile Memory Elements Based on Organic Materials. *Adv. Mater.* **2007**, *19*, 1452−1463.
(8) Cho, B.; Song, S.; Ji, Y.; Kim, T.-W.; Lee, T. Organic Resistive Memory Devices: Performance Enhancement, Integration, and Advanced Architectures. *Adv. Funct. Mater.* **2011**, *21*, 2806−2829.
(9) Ji, Y.; Zeigler, D. F.; Lee, D. S.; Choi, H.; Jen, A. K.-Y.; Ko, H. C.; Kim, T.-W. Flexible and Twistable Non-Volatile Memory Cell Array with All-Organic One Diode−One Resistor Architecture. *Nature Commun.* **2013**, *4*, 2707.
(10) Song, S.; Cho, B.; Kim, T.-W.; Ji, Y.; Jo, M.; Wang, G.; Choe, M.; Kahng, Y. H.; Hwang, H.; Lee, T. Three-Dimensional Integration of Organic Resistive Memory Devices. *Adv. Mater.* **2010**, *22*, 5048−5052.
(11) Kwan, W. L.; Tseng, R. J.; Yang, Y. Multi-Layer Stackable Polymer Memory Devices. *Philos. Trans. R. Soc. A* **2009**, *367*, 4159−4167.
(12) Kim, S.; Jeong, H. Y.; Kim, S. K.; Choi, S.-Y.; Lee, K. J. Flexible Memristive Memory Array on Plastic Substrates. *Nano Lett.* **2011**, *11*, 5438−5442.
(13) Heremans, P.; Gelinck, G. H.; Müller, R.; Baeg, K.-J.; Kim, D.-Y.; Noh, Y.-Y. Polymer and Organic Nonvolatile Memory Devices. *Chem. Mater.* **2011**, *23*, 341−358.
(14) Lin, W.-P.; Liu, S.-J.; Gong, T.; Zhao, Q.; Huang, W. Polymer-Based Resistive Memory Materials and Devices. *Adv. Mater.* **2014**, *26*, 570−606.
(15) Simmons, J. G.; Verderber, R. R. New Conduction and Reversible Memory Phenomena in Thin Insulating Films. *Proc. R. Soc. London, Ser. A* **1967**, *301*, 77−102.
(16) Bozano, L. D.; Kean, B. W.; Deline, V. R.; Salem, J. R.; Scott, J. C. Mechanism for Bistability in Organic Memory Elements. *Appl. Phys. Lett.* **2004**, *84*, 607−609.
(17) Bozano, L. D.; Kean, B. W.; Beinhoff, M.; Carter, K. R.; Rice, P. M.; Scott, J. C. Organic Materials and Thin-Film Structures for Cross-Point Memory Cells Based on Trapping in Metallic Nanoparticles. *Adv. Funct. Mater.* **2005**, *15*, 1933−1939.
(18) Gao, S.; Song, C.; Chen, C.; Zeng, F.; Pan, F. Dynamic Processes of Resistive Switching in Metallic Filament-Based Organic Memory Devices. *J. Phys. Chem. C* **2012**, *116*, 17955−17959.
(19) Jin, Z.; Liu, G.; Wang, J. Organic Nonvolatile Resistive Memory Devices Based on Thermally Deposited Au Nanoparticle. *AIP Adv.* **2013**, *3*, 052113/1−052113/7.
(20) Ouyang, J.; Chu, C.-W.; Szmanda, C. R.; Ma, L.; Yang, Y. Programmable Polymer Thin Film and Non-Volatile Memory Device. *Nat. Mater.* **2004**, *3*, 918−922.
(21) Cario, L.; Vaju, C.; Corraze, B.; Guiot, V.; Janod, E. Electric-Field-Induced Resistive Switching in a Family of Mott Insulators: Towards a New Class of RRAM Memories. *Adv. Mater.* **2010**, *22*, 5193−5197.
(22) Stoliar, P.; Cario, L.; Janod, E.; Corraze, B.; Guillot-Deudon, C.; Salmon-Bourmand, S.; Guiot, V.; Tranchant, J.; Rozenberg, M. Universal Electric-Field-Driven Resistive Transition in Narrow-Gap Mott Insulators. *Adv. Mater.* **2013**, *25*, 3222−3226.
(23) Guiot, V.; Cario, L.; Janod, E.; Corraze, B.; Ta Phuoc, V.; Rozenberg, M.; Stoliar, P.; Cren, T.; Roditchev, D. Avalanche Breakdown in $GaTa_4Se_{8-x}Te_x$ Narrow-Gap Mott Insulators. *Nat. Commun.* **2013**, *4*, 1722.
(24) Dubost, V.; Cren, T.; Vaju, C.; Cario, L.; Corraze, B.; Janod, E.; Debontridder, F.; Roditchev, D. Resistive Switching at the Nanoscale in the Mott Insulator Compound $GaTa_4Se_8$. *Nano Lett.* **2013**, *13*, 3648−3653.
(25) Corraze, B.; Janod, E.; Cario, L.; Moreau, P.; Lajaunie, L.; Stoliar, P.; Guiot, V.; Dubost, V.; Tranchant, J.; Salmon, S.; et al. Electric Field Induced Avalanche Breakdown and Non-Volatile Resistive Switching in the Mott Insulators AM_4Q_8. *Eur. Phys. J.: Spec. Top.* **2013**, *222*, 1046−1056.
(26) Kato, R. Conducting Metal Dithiolene Complexes: Structural and Electronic Properties. *Chem. Rev.* **2004**, *104*, 5319−5346.
(27) Kato, R. Development of π-Electron Systems Based on $[M(dmit)_2]$ (M = Ni and Pd; dmit: 1,3-dithiole-2-thione-4,5-dithiolate) Anion Radicals. *Bull. Chem. Soc. Jpn.* **2014**, *87*, 355−374.
(28) Kobayashi, A.; Fujiwara, E.; Kobayashi, H. Single-Component Molecular Metals with Extended-TTF Dithiolate Ligands. *Chem. Rev.* **2004**, *104*, 5243−5264.
(29) Cui, H. B.; Kobayashi, H.; Ishibashi, S.; Sasa, M.; Iwase, F.; Kato, R.; Kobayashi, A. A Single-Component Molecular Superconductor. *J. Am. Chem. Soc.* **2014**, *136*, 7619−7622.
(30) Zhou, B.; Idobata, Y.; Kobayashi, A.; Cui, H.; Kato, R.; Takagi, R.; Miyagawa, K.; Kanoda, K.; Kobayashi, H. Single-Component Molecular Conductor $[Cu(dmdt)_2]$ with Three-Dimensionally Arranged Magnetic Moments Exhibiting a Coupled Electric and Magnetic Transition. *J. Am. Chem. Soc.* **2012**, *134*, 12724−12731.
(31) Kokatam, S.; Ray, K.; Pap, J.; Bill, E.; Geiger, W. E.; LeSuer, R. J.; Rieger, P. H.; Weyhermüller, T.; Neese, F.; Wieghardt, K. Molecular and Electronic Structure of Square-Planar Gold Complexes Containing Two 1,2-Di(4-*tert*-butylphenyl)ethylene-1,2-dithiolato Ligands: $[Au(^2L)_2]^{1+/0/1-/2-}$. A Combined Experimental and Computational Study. *Inorg. Chem.* **2007**, *46*, 1100−1111.
(32) Schiødt, N. C.; Bjørnholm, T.; Bechgaard, K.; Neumeier, J. J.; Allgeier, C.; Jacobsen, C. S.; Thorup, N. Structural, Electrical, Magnetic, and Optical Properties of Bis-benzene-1,2-dithiolato-Au(IV) Crystals. *Phys. Rev. B* **1996**, *53*, 1773.
(33) Dautel, O. J.; Fourmigué, M.; Canadell, E.; Auban-Senzier, P. Fluorine Segregation Controls the Solid-State Organization and Electronic Properties of Ni and Au Dithiolene Complexes: Stabilization of a Conducting Single-Component Gold Dithiolene Complex. *Adv. Funct. Mater.* **2002**, *12*, 693−698.
(34) Tenn, N.; Bellec, N.; Jeannin, O.; Piekara-Sady, L.; Auban-Senzier, P.; Iniguez, J.; Canadell, E.; Lorcy, D. A Single-Component Molecular Metal Based on a Thiazole Dithiolate Gold Complex. *J. Am. Chem. Soc.* **2009**, *131*, 16961−16967.
(35) Yzambart, G.; Bellec, N.; Nasser, G.; Jeannin, O.; Roisnel, T.; Fourmigué, M.; Auban-Senzier, P.; Íñiguez, J.; Canadell, E.; Lorcy, D. Anisotropic Chemical Pressure Effects in Single-Component Molecular Metals Based on Radical Dithiolene and Diselenolene Gold Complexes. *J. Am. Chem. Soc.* **2012**, *134*, 17138−17148.
(36) A detailed investigation of the temperature dependence of E_{th} is beyond the scope of this paper and will be published elsewhere.
(37) Waser, R.; Aono, M. Nanoionics-Based Resistive Switching Memories. *Nat. Mater.* **2007**, *6*, 833−840.
(38) Sawa, A. Resistive Switching in Transition Metal Oxides. *Mater. Today* **2008**, *11*, 28−36.
(39) Pershin, Y. V.; Di Ventra, M. Memory Effects in Complex Materials and Nanoscale Systems. *Adv. Phys.* **2011**, *60*, 145−227.
(40) Hudgins, J. Wide and Narrow Bandgap Semiconductors for Power Electronics: A New Valuation. *Electron. Mater.* **2003**, *32*, 471−477.
(41) Levinshteĭn, M. E.; Kostamovaara, J.; Vainshtein, S.*Breakdown Phenomena in Semiconductors and Semiconductor Devices*; World Scientific Publishing Co. Pte. Ltd.: Singapore, 2005.
(42) Sabeth, F.; Iimori, T.; Ohta, N. Insulator−Metal Transitions Induced by Electric Field and Photoirradiation in Organic Mott Insulator Deuterated κ-$(BEDT\text{-}TTF)_2Cu[N(CN)_2]Br$. *J. Am. Chem. Soc.* **2012**, *134*, 6984−6986.
(43) Vaju, C.; Cario, L.; Corraze, B.; Janod, E.; Dubost, V.; Cren, T.; Roditchev, D.; Braithwaite, D.; Chauvet, O. Electric-Pulse-Induced Resistive Switching and Possible Superconductivity in the Mott Insulator $GaTa_4Se_8$. *Microelectron. Eng.* **2008**, *85*, 2430−2433.

DOI: 10.1021/jp512810e
J. Phys. Chem. C 2015, 119, 2983−2988

(44) Tranchant, J.; Janod, E.; Corraze, B.; Stoliar, P.; Rozenberg, M.; Besland, M.-P.; Cario, L. Control of Resistive Switching in AM_4Q_8 Narrow Gap Mott Insulators: A First Step towards Neuromorphic Applications. *Phys. Status Solidi A* **2014**, DOI: 10.1002/pssa.201400158.
(45) International Technology Roadmap for Semiconductors (ITRS); http://www.itrs.net/Links/2013ITRS/Home2013.htm.

DOI: 10.1021/jp512810e
J. Phys. Chem. C 2015, 119, 2983−2988